3.6.3 Jet Propulsion Laboratory (JPL)

Introduction

The Jet Propulsion Laboratory is developing an approach to determining ITRF-like terrestrial reference frames based upon the use of a Kalman filter/smoother (Wu et al., 2015). Kalman filters are commonly used for estimating the parameters of some system when a stochastic model of the system is available and when the data contain noise. For the purpose of determining a terrestrial reference frame, the system consists of the positions and velocities of geodetic observing stations and associated EOPs along with their full covariance matrices. The data consist of time series of observed VLBI, SLR, GNSS, and DORIS station positions and EOPs along with the data measurement covariance matrices. In addition, measurements from ground surveys of the positions of reference marks of co-located stations are used to tie the technique-specific station networks to each other. The Kalman filter and smoother for reference frame determination software (KALREF) being developed at JPL combines these measurements to determine ITRF-like reference frames subject to constraints imposed on the allowed evolution of the station positions. KALREF includes options for constraining the stations to move linearly or to move linearly and seasonally. Through the use of stochastic models for the process noise, the station positions can be constrained to exactly follow this linear or linear and seasonal motion (by setting the process noise to zero), to exactly recover the observed station positions (by setting the process noise to a large value), or to follow a smoothed path (by setting the process noise to some intermediate value). The sequential estimation approach to determining terrestrial reference frames that is being developed at JPL has been used to determine JTRF2014, JPL's realization of a terrestrial reference frame using the ITRF2014 input data sets.

Data Sets

Table 1 lists the input data sets that were used to determine JTRF2014. These are the data sets that the IAG Services submitted to the IERS for the determination of ITRF2014. Before using these data sets to determine JTRF2014 they were edited and pre-processed. Because KALREF uses a fixed time step of one week, the daily GNSS station position (but not the EOP) data were averaged to 1-week intervals, as were the session-wise VLBI data. Stations with observing histories less than 2.5 years were removed, as were regional VLBI sessions. And only those GNSS stations that were included in ITRF2008 were used, augmented by additional IGS stations that were not included in ITRF2008, usually because they started observing after 2008. After this data selection process, data from 671 GNSS, 71 SLR, 159 DORIS, and 71 VLBI stations remained.

Table 1: Data Sets Submitted by the IAG Services for ITRF2014 and Used for JTRF2014

SG	TC	Time Span	Solution	TR	# SINEX	# Sites
P	IGS	1994.0 - 2015.1	**V**ariance-**C**ovariance	Daily	7714	1845
R	IVS	1979.5 - 2015.0	**N**ormal **E**quations	Session-Wise	5796	158
L	ILRS	1983.0 - 2015.1	**V**ariance-**C**ovariance	Fortnightly-Weekly (*)	1392	138
D	IDS	1993.0 - 2015.0	**V**ariance-**C**ovariance	Weekly	1140	160
Local Ties			**V**ariance-**C**ovariance	Sporadic	142	

*The SLR data is given at fortnightly intervals before 1993, at weekly intervals thereafter.
SG: space-geodetic data type; P: GNSS; R; VLBI; L: SLR; D: DORIS; TC: technique center; TR: temporal resolution

Outliers were removed after first individually stacking each technique's data by applying intrinsic constraints. After stacking, any observation having an absolute residual greater than 10 cm or a normalized residual greater than 7 sigma (5 sigma for GNSS) was removed. Because the stated formal uncertainties of the observations are generally overly optimistic, the measurement error covariance matrices were scaled by a factor of $(3.07)^2$ for the GNSS data, $(2.98)^2$ for the VLBI data, $(2.61)^2$ for the SLR data, and $(1.36)^2$ for the DORIS data. These variance factors were iteratively determined from the *a posteriori* variance factors obtained from individual stacks of each technique's data and preliminary reference frame solutions.

For the EOPs, daily observations of the x- and y-components of polar motion from all four space-geodetic measurement techniques were used, as were daily observations of the polar motion rates from GNSS, and session-wise observations of UT1 and LOD from VLBI. No editing was done to the EOP data, and the scale factors that were applied to the measurement error covariance matrices of the EOPs were derived from the scale factors that were applied to that technique's station position measurement error covariance matrices.

Both site ties and polar motion data were used to tie the individual technique's station networks together. All of the site ties available for ITRF2008 were used along with the new ties that became available for ITRF2014. The site ties were applied once, at the epoch of the measurement. And the full vector measurement error covariance matrices were used after rescaling them to make the normalized residuals at the co-located sites be less than 4 sigma.

An indication that the station position, EOP, and site tie measurement error covariance matrices have been properly scaled can be obtained by computing the reduced chi-squared of the post-fit residual. If the reduced chi-squared value is close to unity, then the scaled uncertainties are consistent with the post-fit residuals. For JTRF2014, the reduced chi-squared values of the station positions, EOPs, and site ties are 0.93, 1.02, and 1.02, respectively,

indicating that their measurement error covariance matrices have been reasonably adjusted. The total reduced chi-squared value of all the measurements used to determine JTRF2104 was 1.07.

Solution Strategy

After editing and pre-processing, the data sets listed in Table 1 were combined with a Kalman filter to determine JTRF2014. The model for the station position process noise in the Kalman filter included both a deterministic and a stochastic part. The deterministic part consisted of a linear trend and annual and semiannual periodic terms. The linear trend is meant to account for station motion caused by, for example, plate tectonics, glacial isostatic adjustment, etc. The periodic terms are meant to capture the major component of the station motion caused by surface loading. The stochastic part of the process noise model is meant to capture the non-seasonal signals in the station motion caused by surface loading. For that, we used the atmospheric, non-tidal oceanic, and hydrologic loading models available from the IERS Global Geophysical Fluids Center. A best fitting model for a linear trend and annual and semiannual periodic terms was first fit to and removed from the sum of the weekly averaged loading models. Since KALREF assimilates the first difference of the station position data, not the station positions themselves, first differences of the residual loading displacements at each station were formed and the variance of the first-differenced residual computed. These station-dependent variances then formed the stochastic component of the process noise that was used in the Kalman filter. The median variance of the first-differenced residual displacement caused by the sum of atmospheric, non-tidal oceanic, and hydrologic loading was about $(0.9\ \text{mm})^2$ in the north, about $(0.7\ \text{mm})^2$ in the east, and about $(1.7\ \text{mm})^2$ in the vertical.

These values for the variance of the station-dependent process noise were the nominal values used when filtering the station position data between discontinuities. At a discontinuity in the station position the variance was set to a large value, $(5\ \text{m})^2$, in order to allow the Kalman state to follow the jump in station position. After the discontinuity in the station's position it was reset to its nominal value. Discontinuities in station position can be caused by geophysical events such as earthquakes or by man-made events such as equipment changes. Discontinuities in the station position time series were empirically determined using tools available in GIPSY.

For the EOPs, the process noise models consisted of random walks driven by white noise. The variances of the white noise were set to large values in order to accommodate the day-to-day fluctuations in the EOP values.

Following usual practice, the origin of JTRF2014 was determined solely from SLR data and the orientation was constrained by applying a no-net-rotation condition to ITRF2008. The scale was

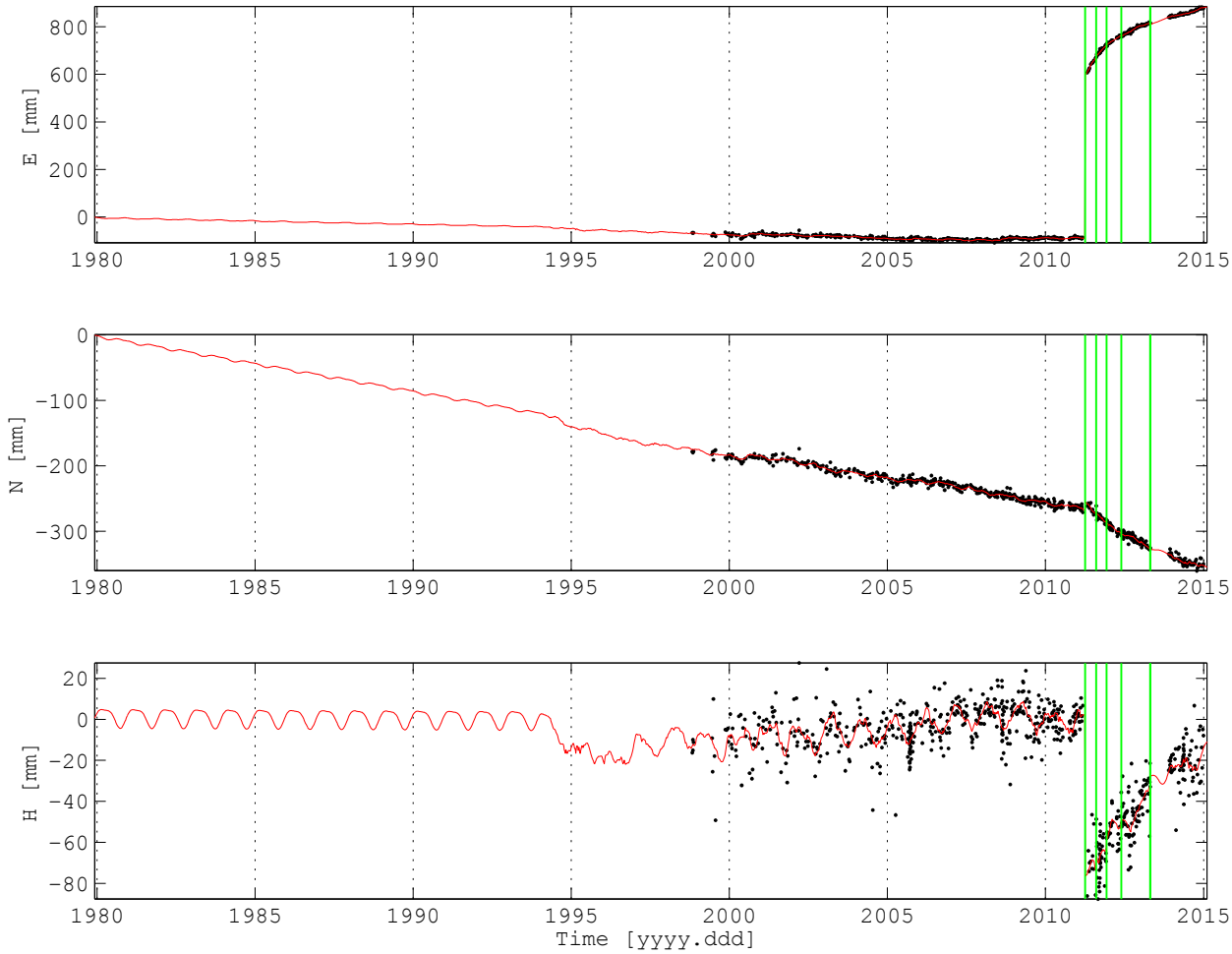

Fig. 1: Observed (black dots) and Kalman-smoothed, interpolated, and extrapolated (red line) position of the VLBI station at Tsukuba, Japan. The vertical green lines indicate the epochs of discontinuities in the observed position of the station. The east, north, and height (or up) component of the station's position are shown in the top, middle, and bottom panels, respectively.

determined from a weighted average of SLR and VLBI data with the weights derived from the weights applied to the SLR and VLBI station position data.

Finally, since stations located near each other can be expected to exhibit the same motion, stations of different techniques that are co-located at the same site were constrained to move together.

JTRF2014

The resulting reference frame, JTRF2014, consists of a set of time series of the positions, but not velocities, of 972 stations spanning November 28, 1979 to February 11, 2015 at weekly intervals along with daily EOPs. As an example of one of the station position time series included in JTRF2014, Figure 1 shows the result for the VLBI station at Tsukuba, Japan. The black dots are the observed positions of the station, the red line is the Kalman-estimated position of the station from JTRF2014, and the vertical green lines

indicate the epochs of the discontinuities in the observed station positions at which the process noise was reset. The coseismic displacement of this station caused by the Tohoku, Japan earthquake of March 11, 2011 is readily apparent, especially in the east (top panel) and up (bottom panel) components. By resetting the process noise to a large value at the epoch of the earthquake, the Kalman-estimated position of the station is able to follow the station's coseismic displacement (red line). Between discontinuities, the nominal value of the process noise at this station causes the Kalman-estimated position to be a smoothed version of the observed position. The deterministic model of the process noise is used to both interpolate across gaps in the observations (such as the gap near 2014) and to extrapolate the position of the station to epochs before the station started observing (such as before 1994) or after the station stopped observing (not shown). Since the VLBI station at Tsukuba is co-located with a GNSS station that started observing before it, and because of the co-motion constraint applied to co-located stations, the Kalman-estimated position of the GNSS station is transferred to the VLBI station at those epochs when the VLBI station was not observing but the GNSS station was. This is most evidently seen in the up component (bottom panel) during 1995 to 1998.

Table 2 compares JTRF2014 to ITRF2014 (Altamimi et al., 2016). The entries in Table 2 are the coefficients of a linear fit to a time series of weekly Helmert transformation parameters that map ITRF2014 to JTRF2014. The ITRF2014 station positions were evaluated at the weekly epoch of the JTRF2014 station positions using the linear velocities reported with ITRF2014. No stations affected by earthquakes were included when computing the Helmert transformation parameters using the projected ITRF2014 station positions. The uncertainties given in parentheses in Table 2 are the 1-sigma formal errors of the linear fit to the weekly Helmert transformation parameters and are hence overly optimistic. The translation (*T*) and rotation (*R*) parameters are all less than 0.8 mm except for T_z. Plots of the weekly T_z Helmert transformation parameter (not shown) indicate greater variability during 1984–1990 which is adversely affecting the linear fit. The scale (*D*) parameter is also larger, but this is to be expected because the JTRF2014 scale comes from a weighted average of the VLBI and SLR data,

Table 2: Helmert transformation parameters mapping ITRF2014 to JTRF2014

		T_x	T_y	T_z	D	R_x	R_y	R_z
	O	-0.57 (0.03)	-0.03 (0.03)	-1.48 (0.04)	-1.64 (0.06)	0.57 (0.02)	0. 75 (0.02)	0.25 (0.02)
	T	-0.12 (0.01)	-0.04 (0.01)	0.19 (0.01)	0.20 (0.01)	0.11 (0.00)	-0.09 (0.00)	-0.17 (0.00)

Units are mm for the offset (O) and mm/yr for the trend (T). The reference epoch for the trend is January 1, 2005. The values in parentheses are the 1-sigma formal errors.

whereas the ITRF2014 scale comes from a simple average of this data. All rate parameters are at most 0.2 mm/yr. Thus, except in scale, JTRF2014 is highly consistent with ITRF2014.

References

Altamimi, Z., P. Rebischung, L. Métivier, and X. Collilieux (2016), ITRF2014: A new release of the International Terrestrial Reference Frame modeling nonlinear station motions, *J. Geophys. Res. Solid Earth*, *121*, doi:10.1002/2016JB013098.

Wu, X., C. Abbondanza, Z. Altamimi, T. M. Chin, X. Collilieux, R. S. Gross, M. B. Heflin, Y. Jiang, and J. W. Parker (2015), KALREF – A Kalman filter and time series approach to the International Terrestrial Reference Frame realization, *J. Geophys. Res. Solid Earth*, *120*(5), 3775–3802, doi:10.1002/2014JB011622.

Richard Gross, Claudio Abbondanza, T. Mike Chin, Mike Heflin, Jay Parker, Xiaoping Wu